

Hydrostatic ^{12}C Burning in CO WDs: the Simmering Phase of SNe Ia Progenitors

Francisco Förster¹, Pierre Lesaffre², and Philipp Podsiadlowski³

¹Departamento de Astronomía, Universidad de Chile, Casilla 36-D, Santiago, Chile
email: francisco.forster@gmail.com

²Laboratoire de Radioastronomie, 24 rue Lhomond, 75231 PARIS Cedex 05, France
email: pierre.lesaffre@lra.ens.fr

³University of Oxford, Department of Physics, Oxford, OX1 3RH, UK
email: podsi@astro.ox.ac.uk

Abstract. Among the possible progenitor scenarios considered for Type Ia supernovae, those that involve a carbon–oxygen white dwarf (CO WD) accreting stably towards the Chandrasekhar mass should undergo a phase of hydrostatic carbon burning under high densities and strong convection: the *simmering* or carbon–flash phase, which can extend for a few hundred years before explosion. During this phase the progenitor CO WD can burn a small fraction of its carbon hydrostatically, releasing energy and ashes that make the star convective and able to capture electrons from the degenerate plasma. In this work we present simplified pre–supernova evolution models of CO WDs growing towards the Chandrasekhar mass accreting matter stably and evolving through the simmering phase towards ignition in order to explore the effects of different initial masses and cooling times in the final chemical composition of the WD before explosion. Preliminary results show that, as expected, denser systems at the start of the simmering phase undergo stronger neutronization. The amount of neutronization is less than what is found in the one–zone models of Chamulak *et al.* (2008), about a third, and can vary by about a factor of two depending on the exact path to explosion.

Keywords. stars: supernova, white dwarfs — nuclear reactions, nucleosynthesis, abundances

1. Introduction

Type Ia supernovae (SNe Ia) are thought to be the thermonuclear explosion of white dwarf stars. Although significant progress has been made understanding the physics and the environments of these explosions, it is not clear what are their exact progenitors. We understand the likely physical origin of the energy displayed in their light curves, the radioactive decay of different amounts of freshly synthesized ^{56}Ni (see e.g. Mazzali *et al.* 1998), and significant progress has been made understanding the composition and velocity structure of their ejecta (Stehle *et al.* 2005, Woosley *et al.* 2007, Mazzali *et al.* 2007). Studying their environments, it has been found that their progenitors are generally older than those of core collapse supernovae and span a wide range of explosion ages (see e.g. Scannapieco & Bildsten 2005), with systems in older environments systematically fainter than those in younger environments (Hamuy *et al.* 1996). Evidence for asymmetries in the inner regions of the ejecta connected to early time diversity of SNe Ia light curves and spectra (Benetti *et al.* 2005, Motohara *et al.* 2006, Maeda *et al.* 2010, Maeda *et al.* 2011), suggests that three dimensional effects are also important.

The consensus seems to be that SNe Ia are the the thermonuclear explosions of carbon–oxygen white dwarf stars (Hillebrandt & Niemeyer 2000), which are expected to leave an homologously expanding ejecta with the following structure: iron group elements (IGEs) in the center that power the light curves via radioactive ^{56}Ni , detected at low

velocities and consistent with the complete burning of carbon and oxygen at relatively high progenitor densities; intermediate mass elements (IMEs) like Si, Mg, S or O found at higher velocities, which is consistent with the partial burning of carbon and oxygen at lower progenitor densities; and, in some cases, unburnt carbon seen at higher velocities and at earlier times (Parrent *et al.* 2011, Folatelli *et al.* 2011), which is consistent with unburnt matter from the outer layers of the progenitor WD.

Observations of the nebular phase of different SNe Ia suggest that significant amount of stable iron group elements are present at low velocities, a signature of Chandrasekhar mass hydrostatic WDs, and that they are off-center with respect to the rest of the ejecta (Motohara *et al.* 2006, Fesen *et al.* 2007, Gerardy *et al.* 2007). The only evolutionary path that has shown to lead to a hydrostatic CO WD close to the Chandrasekhar mass and then an SN Ia is that where a CO WD accretes matter stably from a Roche-lobe filling companion, either a helium star, a main sequence star, a sub-giant star, or a red-giant star, in the so-called *Chandrasekhar mass, single-degenerate* scenario, or SD-M_{Ch}, which is studied in this work (Hachisu, Kato, & Nomoto 1996, Li & van den Heuvel 1997, Hachisu, Kato, & Nomoto 1999, Hachisu *et al.* 1999, Langer *et al.* 2000, Han & Podsiadlowski 2004, Meng, Chen, & Han 2009).

An important requirement for the SD-M_{Ch} scenario is that it should reproduce the observed connection between the properties of the ejecta and the environments of SNe Ia, namely that bright, slow declining SNe Ia occur preferentially in young stellar environments. The stochastic nature of the explosion and orientation effects can naturally give a range of ^{56}Ni masses and observational properties, but the systematic preference of bright systems to occur in young environments means that there must be a systematic connection between pre-supernova evolution and explosion diversity. Furthermore, the SD-M_{Ch} scenario must be able to explain why some systems appear to explode off-center.

2. Path to Type Ia Supernova in the SD Scenario

In the SD-M_{Ch} scenario a CO WD is first formed in a close binary system via binary interactions. When the CO WD is formed it undergoes a *cooling phase*, where its energy is released radiatively at almost constant density for hundreds or thousands of Myr depending on the time remaining for the companion to fill its Roche lobe. As the companion evolves and fills its Roche lobe a *transfer phase* will begin, where matter will be accreted to the CO WD and will lead to thermally stable or unstable burning at its surface depending on the composition of the matter being accreted, the mass transfer rate and the mass and thermal state of the CO WD. It is thought that only when mass transfer is in a narrow range for a given CO WD mass, thermally stable burning can allow the CO WD to grow up to the Chandrasekhar mass (see e.g. Nomoto, Thielemann, & Yokoi 1984, Shen & Bildsten 2007, Nomoto *et al.* 2007). If the mass transfer rate is too low, weak flashes could prevent mass growth; if the mass transfer rate is too high the WD's envelope grows into a red giant solution or becomes the source of strong winds that can in some cases help stabilize the accretion (Hachisu, Kato, & Nomoto 1996, Hachisu, Kato, & Nomoto 1999). If mass transfer is stable, the CO WD can grow in mass and must shrink to keep the hydrostatic equilibrium, and because the accretion time-scale is typically shorter than the star's diffusion time-scale, the star's core compresses adiabatically. This adiabatic compression at the center and heat diffusion from the hot accreting envelope can make the central temperature increase under degenerate conditions.

As the central temperature increases, the WD will start to burn its carbon hydrostatically in the center. Initially, the high central densities will make neutrino cooling dominant over nuclear fusion heating, but as more carbon is burned nuclear heating will

become dominant and the star will be forced to transport the excess central energy convectively, beginning the *simmering phase*, or a *thermonuclear carbon flash*. During this phase the convective core can grow to engulf most of the star by mass in a few hundred years, while the ashes of carbon burning can undergo e^- -capture and β -decays as they move between high and low density regions (see Lesaffre, Podsiadlowski, & Tout 2005 and references therein), in a process known as the *convective Urca process* (see Figure 1).

Finally, when the temperature is high enough, one or more ignition spots will give rise to nuclear flames that will propagate in the highly convective medium, the *thermonuclear runaway*, causing a subsonic deflagration wave to burn the inner region of the star while expanding it, and later possibly transition into a detonation wave.

3. Numerical Experiments of the Simmering Phase

We have performed numerical simulations of the cooling, accretion and simmering phases approaching ignition using the time-dependent theory of convection in Lesaffre, Podsiadlowski, & Tout 2005, with the N1 reaction network of Förster, Lesaffre, & Podsiadlowski 2010 and the FLASH The Tortoise stellar evolution code (Lesaffre *et al.* 2006). Because the e^- -capture time-scales can be similar to the convective turn-over time-scales, it becomes necessary to use modified stellar evolution codes that include self-consistent, time-dependent theories of convection, and in order to achieve numerical stability it becomes necessary to solve the chemistry and structure partial differential equations simultaneously, which requires the use of simplified nuclear reaction networks with sufficient accuracy.

In Figure 1 we show examples of our simulations (see caption for details) in a temperature – electron density diagram ($T - \rho Y_e$). The region where neutronization via e^- -captures dominates is shown at densities higher than the zero-labeled contour in the diagram. Over-plotted are different tracks for the central evolution of CO WDs approaching ignition and different profiles for a particular case approaching ignition.

These experiments are an extension of the work of Lesaffre *et al.* 2006, but with an improved reaction network that takes into account e^- -captures and β -decays. We are not including chemical potential changes in the energy equation due to numerical difficulties, so these experiments should be taken only as an estimation of the amount of neutronization during the simmering phase, and should not be taken as the solution to the convective Urca process problem.

These simulations show that long time-delay scenarios of initially more massive CO WDs result in stronger neutronization during the simmering phase because their convective cores will be located mainly in high density regions where e^- -captures dominate (Figure 1). Interestingly, long time-delay scenarios are predicted to come from initially more massive CO WDs (Meng, Yang, & Li 2010), suggesting the generalization that older SNe Ia progenitors come from denser and more neutron-rich progenitors. Moreover, Townsley *et al.* (2007) suggests that denser systems synthesize lower ^{56}Ni masses systematically during the explosion, confirming that the SD- M_{Ch} scenario could reproduce the observed diversity among galaxy types.

In Figure 2 and Figure 3 we show two preliminary examples of the chemical evolution during the simmering phase that confirms that denser systems during simmering undergo stronger neutronization. The chemical profiles in Figure 2 show that: (1) because of the high central densities ^{23}Ne becomes the main source of neutrons, about four times the neutrons provided by ^{13}C , and (2) because of ^{12}C -burning the mass fraction of ^{23}Ne is significantly higher than the pre-burning ^{23}Na mass fraction. The chemical profiles in Figure 3 show that: (1) the amount of neutronization is about half of that in Figure 2

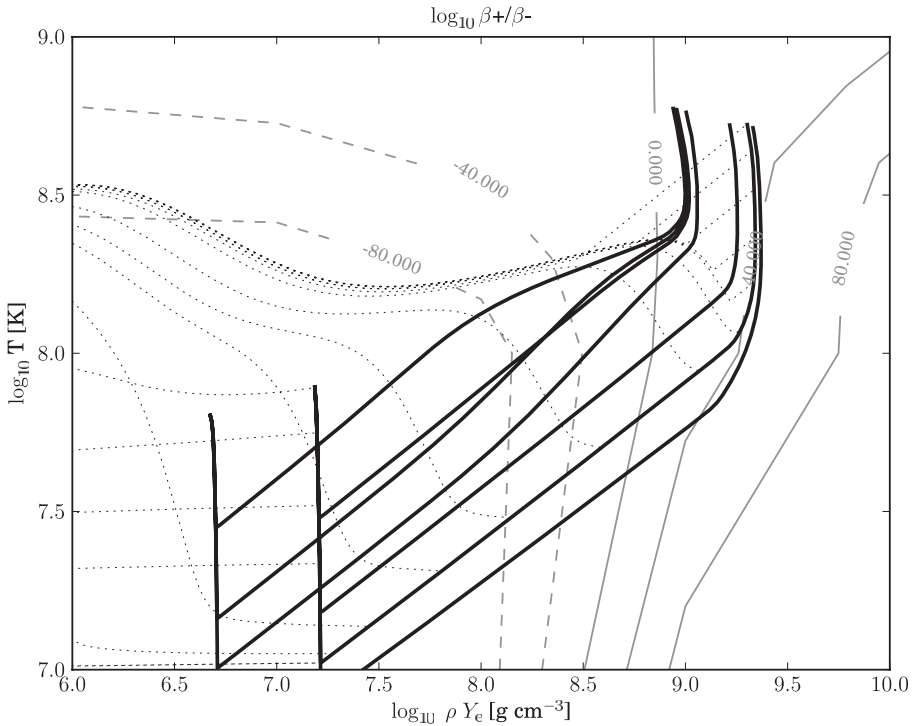


Figure 1. Temperature vs electron density (ρY_e) diagram in the range relevant for the simmering phase of hydrostatic CO WDs near the Chandrasekhar mass. Gray contours correspond to the logarithm of the ratio between the rates of ^{23}Na e^- -captures onto ^{23}Ne and ^{23}Ne β -decays onto ^{23}Na , showing that the former is faster at high densities and that the critical line that divides e^- -capture from β -decay dominated regions depends mainly on ρY_e . Note that ^{23}Na is one of the ashes left by ^{12}C -burning during the simmering phase. Thick continuous lines are central $T - \rho Y_e$ tracks for different CO WD reaching the Chandrasekhar mass after cooling and accretion. The three tracks starting at lower densities correspond to an initially $0.8 M_\odot$ CO WD that cools for 100 Myr, 500 Myr and 1 Gyr before accretion (from top to bottom) and the four tracks starting at higher densities correspond to an initially $1.0 M_\odot$ CO WD that cools for 100 Myr, 500 Myr, 1 Gyr and 10 Gyr before accretion (from top to bottom). Dotted lines are $T - \rho Y_e$ profiles for an initially $1.0 M_\odot$ CO WD that cools down for 1 Gyr before accretion. These profiles show how the WD initially cools down to an almost isothermal core, then how the central regions compress and heat adiabatically while from the hot envelope a diffusion wave moves inwards during accretion, and later how the convective core is formed during the simmering phase. It can be seen that during the simmering phase (high density adiabatic profile) the convective core can engulf regions where both e^- -captures or β -decays dominate, which is the cause of the convective Urca process. Lower central densities during the simmering phase produce more β -decay dominated convective cores at ignition. Note that ignition is not reached in these simulations due to numerical difficulties (c.f. Lesaffre *et al.* 2006).

($\approx 3 \times 10^{-4}$ vs. 6×10^{-4}) and (2) because of the low densities, most of the the ^{23}Ne has β -decayed back to ^{23}Na , which contributes with only as many neutrons as ^{13}C . The total amount of neutronization in Figure 2 and 3 is approximately lower by a factor of three than the amount of neutronization found in Chamulak *et al.* (2008), although our calculations have not reached ignition due to numerical difficulties when the time-step between solutions becomes similar to the convective turn-over time-scale.

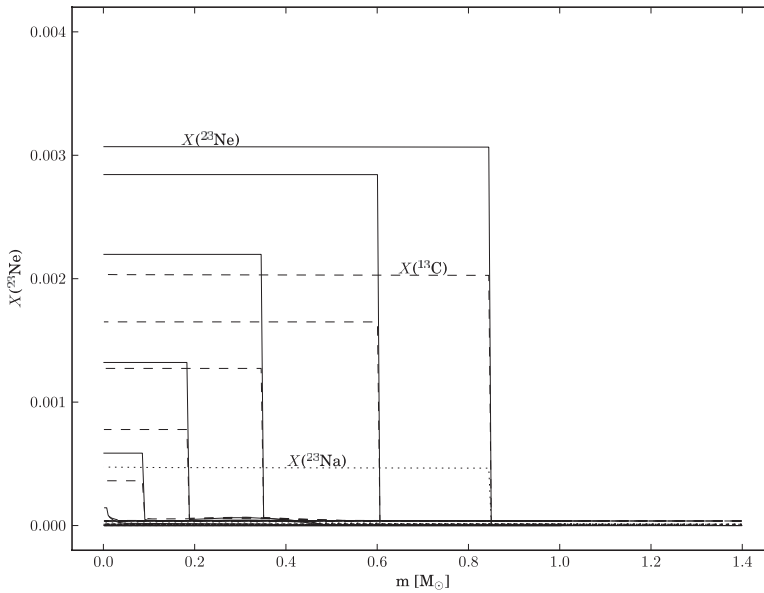


Figure 2. Mass fraction profiles of the main neutron-rich species ^{23}Ne (continuous), ^{23}Na (dotted) and ^{13}C (dashed) during the simmering phase of a CO WD that reached the Chandrasekhar mass after a 1 Gyr cooling phase with an initial mass of a $1.0 M_{\odot}$. As the convective core grows, ^{12}C is burned into ^{23}Na and ^{20}Ne , the former of which captures electrons into ^{23}Ne at high densities. A sequence of $T - \rho Y_e$ profiles for this particular CO WD is shown in Figure 1.

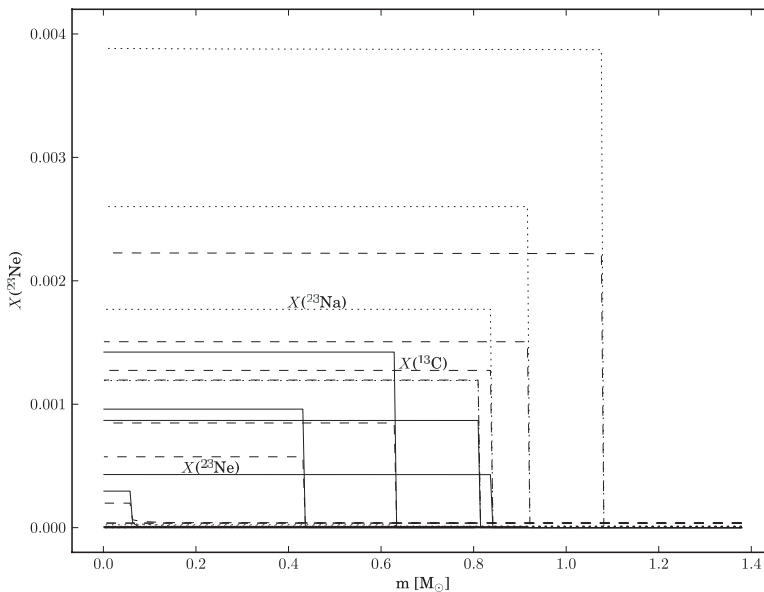


Figure 3. Same as Figure 2, but for an initial mass of $0.8 M_{\odot}$ CO WD and a 500 Myr cooling phase. In this case the convective core extends significantly into low density regions that make the initial neutronization into ^{23}Ne reverse back to ^{23}Na , although without affecting the neutronization into ^{13}C , whose contribution to the total neutronization becomes as important as that of ^{23}Na .

4. Conclusions and Discussion

We have performed numerical experiments of the neutronization occurring during the simmering phase in hydrostatic CO WDs approaching the Chandrasekhar mass in the single degenerate scenario using a new simplified reaction network designed for this purpose (Förster, Lesaffre, & Podsiadlowski 2010). We have found a total neutronization slightly smaller than that found in Chamulak *et al.* (2008), similar to about a third the neutronization that occurs before the WD formation (Timmes, Brown, & Truran 2003) at solar metallicity. Since the cosmological SNe Ia sample is expected to occur in preferentially lower metallicity galaxies, the neutronization during the simmering phase could be dominant in high redshift SNe Ia given the expected metallicity evolution of the hosts (Sullivan *et al.* 2010), although more detailed simulations of the convective Urca process should be performed to better quantify this possibility.

Understanding the convective Urca process remains a key aspect missing from Chandrasekhar mass hydrostatic CO WDs models for progenitors of SNe Ia, as well as for the application of SNe Ia to precision cosmology. This process remains a numerically challenging phase of evolution in spite of several past and present attempts to model it (see e.g. Iben 1978, Iben 1982).

Acknowledgments

F.F. acknowledges support provided by FONDECYT through grant 3110042.

References

- Benetti S., Cappellaro E., Mazzali P. A., *et al.*, 2005, *ApJ*, 623, 1011
 Chamulak D. A., Brown E. F., Timmes F. X., & Dupczak K., 2008, *ApJ*, 677, 160
 Fesen R. A., Höflich P. A., Hamilton A. J. S., Hammell M. C., Gerardy C. L., Khokhlov A. M., & Wheeler J. C., 2007, *ApJ*, 658, 396
 Folatelli G., Phillips M. M., Morrell N., *et al.*, 2011, arXiv, arXiv:1110.3789
 Förster F., Lesaffre P., & Podsiadlowski Ph., 2010, *ApJS*, 190, 334
 Gerardy C. L., Meikle W. P. S., Kotak R., *et al.*, 2007, *ApJ*, 661, 995
 Hachisu I., Kato M., & Nomoto K., 1996, *ApJ*, 470, L97
 Hachisu I., Kato M., & Nomoto K., 1999, *ApJ*, 522, 487
 Hachisu I., Kato M., Nomoto K., & Umeda H., 1999, *ApJ*, 519, 314
 Han Z. & Podsiadlowski P., 2004, *MNRAS*, 350, 1301
 Hamuy M., Phillips M. M., Suntzeff N. B., Schommer R. A., Maza J., & Aviles R., 1996, *AJ*, 112, 2391
 Hillebrandt W. & Niemeyer J. C., 2000, *ARA&A*, 38, 191
 Iben I., Jr., 1978, *ApJ*, 226, 996
 Iben I., Jr., 1982, *ApJ*, 253, 248
 Langer N., Deutschmann A., Wellstein S., & Höflich P., 2000, *A&A*, 362, 1046
 Lesaffre P., Podsiadlowski Ph., & Tout C. A., 2005, *MNRAS*, 356, 131
 Lesaffre P., Han Z., Tout C. A., Podsiadlowski Ph., & Martin R. G., 2006, *MNRAS*, 368, 187
 Li X.-D. & van den Heuvel E. P. J., 1997, *A&A*, 322, L9
 Maeda K., Benetti S., Stritzinger M., *et al.*, 2010, *Natur*, 466, 82
 Maeda K., Leloudas G., Taubenberger S., *et al.*, 2011, *MNRAS*, 413, 3075
 Mazzali P. A., Cappellaro E., Danziger I. J., Turatto M., & Benetti S., 1998, *ApJ*, 499, L49
 Mazzali P. A., Röpke F. K., Benetti S., & Hillebrandt W., 2007, *Sci*, 315, 825
 Meng X., Chen X., & Han Z., 2009, *MNRAS*, 395, 2103
 Meng X.-C., Yang W.-M., & Li Z.-M., 2010, *RAA*, 10, 927
 Motohara K., Maeda K., Gerardy C. L., *et al.*, 2006, *ApJ*, 652, L101
 Nomoto K., Thielemann F.-K., & Yokoi K., 1984, *ApJ*, 286, 644

- Nomoto K., Saio H., Kato M., & Hachisu I., 2007, *ApJ*, 663, 1269
- Pakmor R., Kromer M., Röpke F. K., Sim S. A., Ruiter A. J., & Hillebrandt W., 2010, *Natur*, 463, 61
- Parrent J. T., Thomas R. C., Fesen R. A., *et al.*, 2011, *ApJ*, 732, 30
- Scannapieco E. & Bildsten L., 2005, *ApJ*, 629, L85
- Schwarzschild M. & Härm R., 1965, *ApJ*, 142, 855
- Shen K. J. & Bildsten L., 2007, *ApJ*, 660, 1444
- Sim S. A., Röpke F. K., Hillebrandt W., Kromer M., Pakmor R., Fink M., Ruiter A. J., & Seitenzahl I. R., 2010, *ApJ*, 714, L52
- Stehle M., Mazzali P. A., Benetti S., & Hillebrandt W., 2005, *MNRAS*, 360, 1231
- Sullivan M., Conley A., Howell D. A., *et al.*, 2010, *MNRAS*, 406, 782
- Timmes F. X., Brown E. F., & Truran J. W., 2003, *ApJ*, 590, L83
- Townsley, D. M., Calder, A. C., Asida, S. M., Seitenzahl, I. R., Peng, F., Vladimirova, N., Lamb, D. Q., & Truran, J. W., 2007, *ApJ*, 668, 1118
- Woosley S. E., Kasen D., Blinnikov S., & Sorokina E., 2007, *ApJ*, 662, 487